



## Decay of high spin microsecond isomers in $^{129}\text{In}$ , $^{129}\text{Sn}$ and $^{130}\text{Sb}$ nuclei

J. Genevey, J.A. Pinston, H. Faust, A. Scherillo, G.S. Simpson, I.  
Tsekhanovich

### ► To cite this version:

J. Genevey, J.A. Pinston, H. Faust, A. Scherillo, G.S. Simpson, et al.. Decay of high spin microsecond isomers in  $^{129}\text{In}$ ,  $^{129}\text{Sn}$  and  $^{130}\text{Sb}$  nuclei. International Conference on Fission and Properties of Neutron Rich Nuclei 3, Nov 2002, Sanibel Island, United States. pp.47-54. in2p3-00020016

**HAL Id: in2p3-00020016**

**<https://hal.in2p3.fr/in2p3-00020016>**

Submitted on 16 Jan 2004

**HAL** is a multi-disciplinary open access archive for the deposit and dissemination of scientific research documents, whether they are published or not. The documents may come from teaching and research institutions in France or abroad, or from public or private research centers.

L'archive ouverte pluridisciplinaire **HAL**, est destinée au dépôt et à la diffusion de documents scientifiques de niveau recherche, publiés ou non, émanant des établissements d'enseignement et de recherche français ou étrangers, des laboratoires publics ou privés.

# DECAY OF HIGH SPIN MICROSECOND ISOMERS IN $^{129}\text{In}$ , $^{129}\text{Sn}$ AND $^{130}\text{Sb}$ NUCLEI

J. GENEVEY AND J. A. PINSTON

*Institut des Sciences Nucléaires IN2P3-CNRS/ Université Joseph Fourier,  
F-38026 Grenoble Cedex, France*

H. FAUST, A. SCHERILLO, G. SIMPSON AND I. TSEKHANOVICH

*Institut Laue-Langevin, F-38042 Grenoble Cedex, France*

In this work microsecond isomers of the three nuclei  $^{129}\text{In}$ ,  $^{129}\text{Sn}$ , and  $^{130}\text{Sb}$  were investigated. These nuclei were produced by the thermal-neutron-induced fission of  $^{239}\text{Pu}$  and  $^{241}\text{Pu}$ . The detection is based on time correlation between fission fragments selected by the LOHENGRIN spectrometer at the ILL (Grenoble) and the  $\gamma$  rays or conversion electrons from the isomers. The interpretations of the level schemes are mainly based on a truncated shell model calculation using empirical two body interactions. Several new B(E2) strengths of isomeric transitions were measured and are discussed in the paper.

## 1. Introduction

During the last few years there has been significant progress in the experimental study of the high-spin yrast excitations in neutron rich nuclei with few particles or holes outside the doubly magic  $^{132}\text{Sn}$  and for a neutron number  $N \leq 82$  <sup>1,2,3</sup>. The attention has been focussed on these nuclei because their yrast levels are expected to have a particularly simple structure for testing the basic ingredients of the nuclear shell model, such as the two-body matrix elements of the residual interactions. In this paper we have extended these previous investigations to the three neutron hole  $^{129}_{49}\text{In}$ ,  $^{129}_{50}\text{Sn}$ , and  $^{130}_{51}\text{Sb}$  nuclei.

## 2. Experimental procedure

The nuclei of the A=129 and 130 mass chains were produced by thermal-neutron-induced fission of  $^{239}\text{Pu}$  and  $^{241}\text{Pu}$  targets. The LOHENGRIN spectrometer at the ILL has been used to separate the fission fragments (FF) recoiling from thin targets of about  $400 \mu\text{g}/\text{cm}^2$ , according to their

A/q ratios. The FF are detected by a  $\Delta E$  gas detector, and subsequently stopped in a Mylar foil 12  $\mu\text{m}$  thick. The  $\gamma$ -rays deexciting the isomeric states are detected by two large-volume Ge detectors and the conversion electrons are detected by two cooled adjacent Si(Li) detectors covering a total area of  $2 \times 6 \text{ cm}^2$  and located at 7 mm behind the Mylar window. The electron detection efficiency is very high, about 30%. The gas pressure of the ionization chamber was tuned to stop the FF at about 2  $\mu\text{m}$  from the outer surface of the Mylar window to minimize electron absorption and to have good energy resolution. With this set-up, it is possible to detect conversion electrons down to about 15 keV. Note that a very low energy-detection threshold and a very high detection efficiency are absolutely necessary to observe the very low energy isomeric transitions expected in nuclei close to doubly-magic systems.

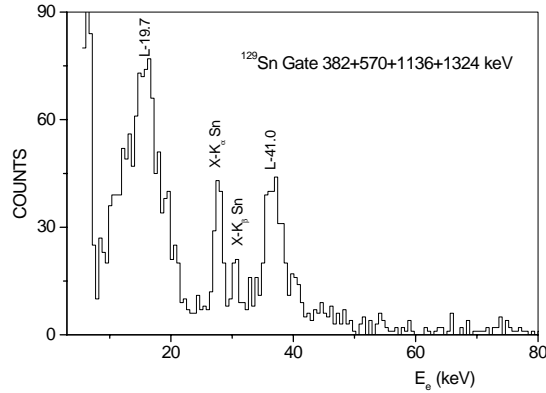


Figure 1. Si(Li) spectrum of  $^{129m}\text{Sn}$  gated by the sum of the 382, 570, 1136 and 1324 keV  $\gamma$ -rays.

### 3. Theoretical calculations

A semi-empirical shell model calculation was performed using the OXBASH<sup>4</sup> code. A truncated configuration was used including only the orbitals  $\pi g_{9/2}$  or  $\pi g_{7/2}$  for the proton and  $\nu d_{3/2}$  and  $\nu h_{11/2}$  for the neutrons. The details concerning the calculations of the energy levels are given in<sup>3</sup>. The two-body matrix elements of the residual interaction were extracted,

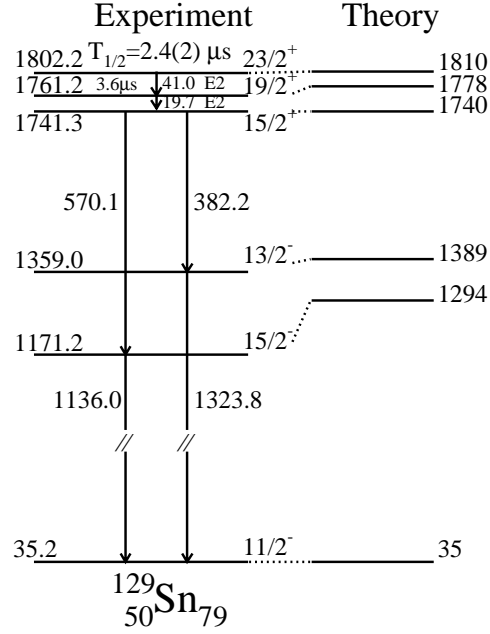


Figure 2. Decay scheme of the  $^{129}\text{Sn}$  isomers. The calculated energies are given relative to the low-lying  $11/2^-$  state at 35 keV.

wherever possible, from experimental data. However, the complete experimental data are not available for the n-p interactions and we have used the calculated values of Andreozzi et al. <sup>5</sup> for the  $\pi g_{7/2}\nu h_{11/2}$  configuration and the values of Van Maldeghem et al. <sup>6</sup> for the  $\pi g_{9/2}\nu h_{11/2}$  configuration. Only yrast or near yrast states having rather pure configurations are considered in the calculation. A comparison between the experimental levels of  $^{129}\text{Sn}$ ,  $^{130}\text{Sb}$  and  $^{129}\text{In}$  and the calculations is shown in Fig. 2, 3 and 5 respectively.

## 4. Results

### 4.1. $^{129}_{50}\text{Sn}$

The Si(Li) spectrum in coincidence with the four  $\gamma$  rays of  $^{129}\text{Sn}$  is shown in Fig. 1. In addition to the Sn  $K_\alpha$  and  $K_\beta$  X-rays, the L-conversion elec-

trons of a 41.0 keV transition and the L-conversion electrons of a 19.7 keV transition are also observed. Two different values of  $2.4(2) \mu\text{s}$  and  $3.6(2) \mu\text{s}$  are measured for the 41.0 keV transition, and for the 19.7 keV transition as well as for the  $\gamma$  rays, respectively. Hence, two  $\mu\text{s}$  isomers in cascade are present in  $^{129}\text{Sn}$ . The relative intensities of the two isomeric transitions show that the 41.0 keV transition is above the 19.7 keV one.

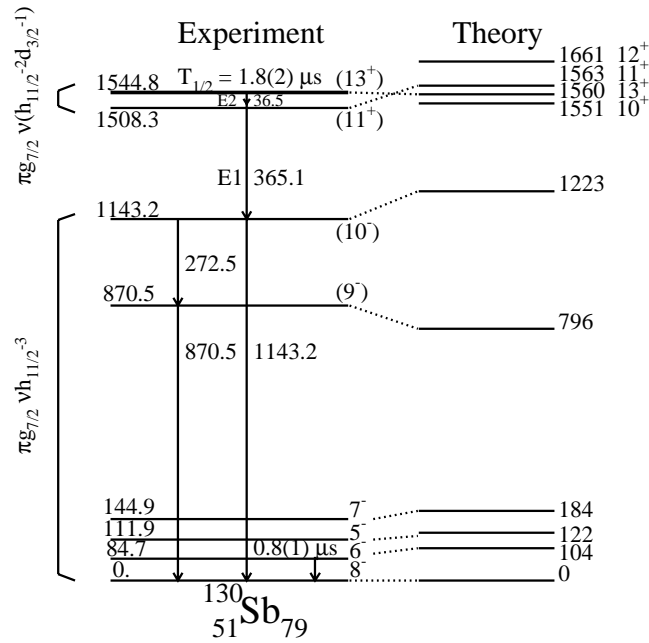


Figure 3. Decay scheme of the  $^{130}\text{Sb}$  isomer. The theoretical energies are determined relative to the  $8^-$  ground state. The two negative parity states at 111.9 and 144.9 keV are from Ref.<sup>7</sup>.

The level scheme of  $^{129}\text{Sn}$  is shown in Fig. 2. The two  $19/2^+$  and  $23/2^+$  isomers in cascade in  $^{129}\text{Sn}$  are well reproduced by the model which shows that the  $\nu(h_{11/2}^{-2}d_{3/2}^{-1})$  is the leading configuration of these states. The negative parity states belong to the  $\nu h_{11/2}^{-3}$  configuration. However, the fully aligned  $27/2^-$  state of that configuration was not observed in this experiment. May be its half-life is too short as discussed in Ref. <sup>2</sup> and it decays during its  $2.2 \mu\text{s}$  flight time through the LOHENGRIN spectrometer.

#### 4.2. $^{130}_{50}\text{Sb}$

The odd-odd  $^{130}\text{Sb}$  nucleus has the same number of neutrons and one more proton than  $^{129}\text{Sn}$ . A new isomer of 1.8  $\mu\text{s}$  half-life, decaying by a low-energy E2 transition of 36.5 keV energy, was observed. The conversion electrons of another isomeric transition were also observed in the Si(Li) spectrum; they correspond to the already known  $6^- \rightarrow 8^-$  E2 transition <sup>7</sup>. A value of  $T_{1/2}=0.8(1)$   $\mu\text{s}$  was measured for its half-life for the first time.

The decay scheme of the new isomer of  $^{130}\text{Sb}$  is shown in Fig. 3. The first excited state at 870.5 keV is the unique overlap between the levels fed by the microsecond isomer and the levels fed by  $\beta$ -decay. However, this level which feeds exclusively the  $8^-$  ground state and not the  $6^-$  state at 84.7 keV has very likely a spin and parity value  $I^\pi=9^-$  and not the value  $I^\pi=7^-$  previously proposed by Walters et al. <sup>7</sup>. The level scheme proposed supposes that the levels are close to the yrast line, as in the other microsecond isomers in this mass region fed by fission.

In  $^{130}\text{Sb}$ , the calculation shows that the  $10^+$ ,  $11^+$  and  $13^+$  states of the  $\pi g_{7/2}\nu(h_{11/2}^{-2}d_{3/2}^{-1})$  configuration are all in an energy range of only 12 keV. This result provides strong support for an isomeric  $13^+ \rightarrow 11^+$  transition of very low energy and E2 multipolarity, although the precision of the calculation is not sufficient to reproduce the observed order of the levels. This  $13^+$  isomer in  $^{130}\text{Sb}$  is the analogous to the  $19/2^+$  isomer in  $^{129}\text{Sn}$  and in fact, they have comparable excitation energies 1545 and 1761 keV respectively, in these two nuclei.

The negative parity states belonging to the  $\pi g_{7/2}\nu(h_{11/2}^{-3})$  configuration are well reproduced by the model. In the absence of more complete experimental data in  $^{132}\text{Sb}$ , this feature shows *a posteriori* that the realistic effective interaction derived from the Bonn potential and used by Andreozzi et al. reproduces correctly the n-p  $\pi g_{7/2}\nu h_{11/2}^{-1}$  interaction.

#### 4.3. $^{129}_{49}\text{In}$

The nuclear structure information on the heavy In isotopes is very scarce. The most important results were the possible evidence by Fogelberg et al. <sup>8</sup> of the high-spin yrast-traps  $23/2^-$  and  $29/2^+$  in  $^{129}\text{In}$ , belonging to the aligned configurations  $(\pi g_{9/2}^{-1}\nu(h_{11/2}^{-1}d_{3/2}^{-1}))23/2^-$  and  $(\pi g_{9/2}^{-1}\nu(h_{11/2}^{-2}))29/2^+$  respectively.

In this work, we have observed a new 7.3 (5)  $\mu\text{s}$  isomer in  $^{129}\text{In}$  decaying by four  $\gamma$ -rays of 333.5, 358.9, 995.2 and 1354.0 keV energy. The K-shell conversion electrons of the 333.5 keV transition was also observed in the

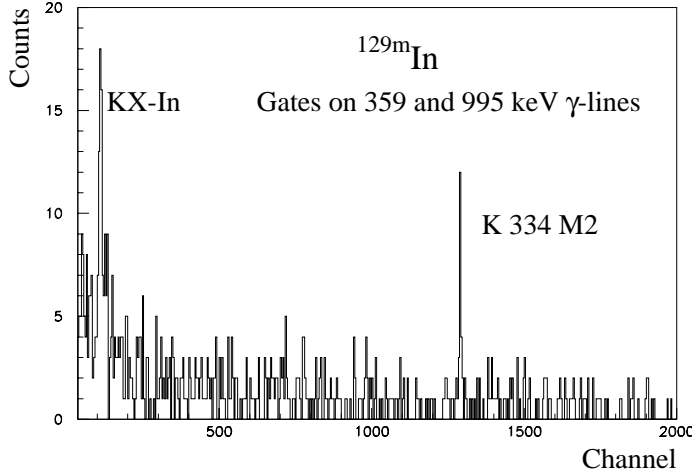


Figure 4. Si(Li) spectrum of  $^{129m}\text{In}$  gated by the sum of 359 and 995 keV  $\gamma$ -rays.

Si(Li) spectrum and shown in Fig. 4. The computed conversion coefficient is compatible with either M2 or E3, but its lifetime is characteristic of M2 as suggested by its reduced transition probability  $B(\text{M2}) = 0.038 \text{ W. u.}$

In Fig. 5 the level scheme of the  $^{129}\text{In}$  nucleus obtained in this work is compared with a theoretical calculation, where only the positive parity states belonging to the  $\pi g_{9/2}^{-1} \nu h_{11/2}^{-2}$  were computed. Good agreement is obtained between the experiment data and theory, and the splitting between the  $11/2^+$  and  $13/2^+$  states is well reproduced. The isomeric state belongs to the  $\pi g_{9/2}^{-1} \nu (h_{11/2}^{-1} d_{3/2}^{-1})$  configuration.

## 5. E2 transition rates in Sn isotopes

In Fig. 6 are plotted the  $B(E2, 19/2^+ \rightarrow 15/2^+)$  and  $B(E2, 23/2^+ \rightarrow 19/2^+)$  values for the odd Sn isotopes as well as the  $B(E2, 10^+ \rightarrow 8^+)$  values for the even Sn isotopes against the mass number  $A$ ; the first two correspond to the transitions involving states of the  $\nu (h_{11/2}^2 d_{3/2})$  configuration, and the last corresponds to the transitions involving states of the  $\nu h_{11/2}^2$  configuration. The data for  $^{129}\text{Sn}$  are from the present work, while the other values have been taken from the literature<sup>9,10,11,12</sup>. The  $B(E2)$  values in the odd and even Sn nuclei show the same trend : a strong

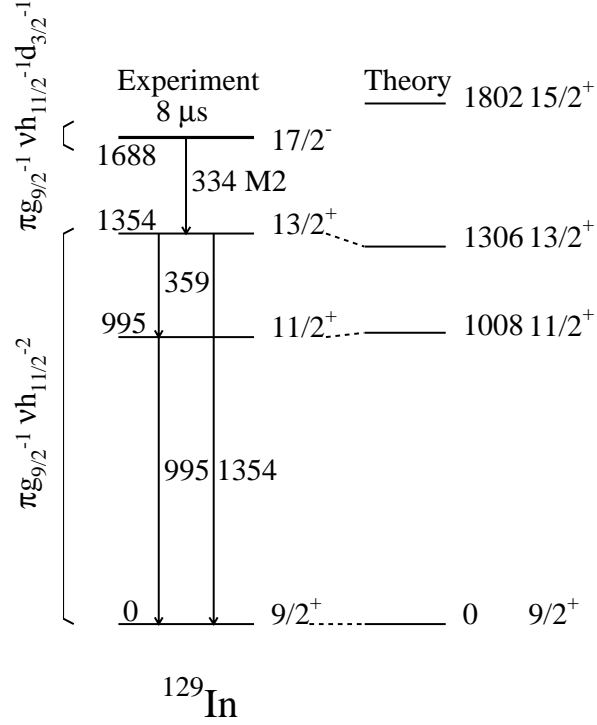


Figure 5. Decay scheme of the  $^{129}\text{In}$  isomer. The theoretical energies are determined relative to the  $9/2^+$  ground state.

decrease of the E2 strength when A decreases, with a deep minimum at A=123. This behavior reflects the filling of the  $\nu h_{11/2}$  neutron subshell and the minimum corresponds to its half filling, which means that for the neutron number N=73 in the Sn isotopes, 6 neutrons occupy the  $\nu h_{11/2}$  orbital. Note that the increase in the B(E2) strength above the deep minimum is much more dramatic for the levels of the  $\nu(h_{11/2}^2 d_{3/2})$  configuration than for the states belonging to the configurations involving the  $\nu h_{11/2}$  orbital only. It is a challenge for the future to complete the data of the  $\nu(h_{11/2}^2 d_{3/2})$  configuration below A=123 where an increase in the B(E2) values is expected.

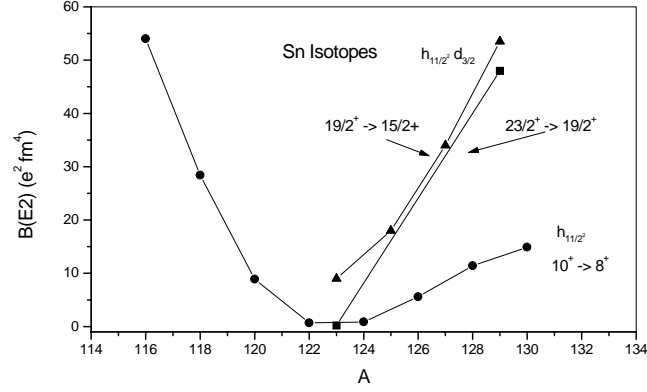


Figure 6.  $B(E2)$  values of even and odd Sn isotopes involving the  $\nu(h_{11/2}^2)$  and  $\nu(h_{11/2}^2 d_{3/2})$  configuration respectively.

## References

1. P. Bhattacharyya et al., Phys. Rev. Lett. **87**, 062502 (2001).
2. J. A. Pinston et al., Phys. Rev. C **61**, 024312 (2000).
3. J. Genevey et al., Eur. Phys. J. A **9**, 191 (2000).
4. B. A. Brown, A. Etchegoyen, and W. D. H. Rae OXBASH (1984) unpublished.
5. F. Andreozzi et al., Phys. Rev. C **59**, 746 (1999).
6. J. Van Maldeghem, Phys. Rev. C **32**, 1067 (1985).
7. W. B. Walters, and C. A. Stone, Proc. Intern. Workshop Nucl. Fission and Fission Product Spectroscopy, edited by H. Faust and G. Fioni, Seyssins, France, p. 182 (1994).
8. B. Fogelberg et al., Intern. Workshop Nucl. Fission and Fission Product Spectroscopy, 2nd, Seyssins, France, edited by H. Faust and G. Fioni and F.-J. Hambsch, AIP Conf. Proc. 447, p. 191, (1998).
9. B. Fogelberg et al., Nucl. Phys. **A352**, 157 (1981).
10. R. Broda et al., Phys. Rev. Lett. **68**, 1671 (1992).
11. J. Genevey et al., AIP Conf. Proc. No. 455 (AIP, Woodbury, NY, 1998) p. 694.
12. C. T. Zhang et al., Phys. Rev. C **62**, 057305 (2000).